Journal of Food Engineering 404 (2026) 112767

Contents lists available at ScienceDirect

Journal of Food Engineering

journal homepage: www.elsevier.com/locate/jfoodeng

Enhancing carob flour (*Ceratonia siliqua* L.) for by-product utilization in food industries: Carob syrup production, functional profiling and application

Ana Martins Vilas-Boas [a], María Emilia Brassesco [a,*], Andreia C. Quintino [b], Bruno Medronho [c,e], Margarida C. Vieira [b,c], Teresa R.S. Brandão [a], Cristina L.M. Silva [a], Beatriz Silva [d], Miguel Azevedo [d], Manuela Pintado [a]

[a] Universidade Católica Portuguesa, CBQF—Centro de Biotecnologia e Química Fina, Laboratório Associado, Escola Superior de Biotecnologia, Rua Diogo Botelho 1327, 4169-005, Porto, Portugal
[b] Department of Food Engineering, High Institute of Engineering, University of Algarve, Campus da Penha, 8000-139, Faro, Portugal
[c] MED—Mediterranean Institute for Agriculture, Environment and Development & Change—Global Change and Sustainability Institute, Instituto Superior de Engenharia, Universidade do Algarve, Campus da Penha, 8005-139, Portugal
[d] Decorgel, Rua do Progresso, 363, Lantemil, 4785-647, Trofa, Portugal
[e] FSCN Research Center, Surface and Colloid Engineering, Mid Sweden University, SE-851 70, Sundsvall, Sweden

ARTICLE INFO

Keywords:
Legume
Modification
Thermal hydrolysis
Enzymatic hydrolysis
Valorization

ABSTRACT

The focus on by-product valorization in the food industry, particularly from the carob pod, underscores a commitment to sustainability and resource efficiency. This fruit, sourced from the leguminous evergreen carob tree (Ceratonia siliqua L.), is renowned for its adaptable flavour and nutritional value, in Mediterranean regions such as Portugal. Its production yields significant by-products, presenting environmental challenges when not managed efficiently. Innovative approaches, including integral carob flour production, aim to optimize utilization while minimizing waste and energy consumption. This study repurposed carob waste to produce novel, value-added ingredients like carob syrup, by thermal hydrolysis of integral carob flour using water at 1:3 solid-to-liquid ratio - obtaining up to 50 % solubility yield. The resulting syrup exhibited 72 % °Brix, a melting temperature (Tm) of approximately 130 °C and predominantly viscous behavior with minimal elastic (solid-like) response. Lastly, the syrup was incorporated into a carob-based brigadeiro, replacing conventional glucose-fructose syrup. Simulated gastrointestinal digestion revealed enhanced bioaccessibility of sugars and phenolics, and increased antioxidant activity during the intestinal phase. Despite sugar availability, the prebiotic activity of the syrup decreased when embedded in the brigadeiro matrix, potentially due to interactions with polyphenols or organic acids. Cytotoxicity and permeability assays confirmed safety at ≤0.5 % (w/v) and supported intestinal barrier integrity. These findings support the use of integral carob flour for producing multifunctional ingredients, contributing to circular economy models while meeting consumer demands for healthier, sustainable food products.

1. Introduction

In the food industry, by-product valorization has gained significant attention as a sustainable approach to reduce waste and maximize resource utilization. Carob fruit originates from the carob tree a leguminous evergreen tree (*Ceratonia siliqua* L.) cultivated in the Mediterranean area, namely in Portugal (Papaefstathiou et al., 2018). It is a versatile and nutritious crop and has long been cherished for its sweet, cocoa-like flavor and health benefits (Loullis and Pinakoulaki, 2018; Nasar-abbas et al., 2016; Vilas-Boas et al., 2022) However, the production process often generates a substantial amount of by-products (such as carob pods, seeds, etc.) that, if not properly managed, can pose environmental challenges (Brassesco et al., 2021). To address this issue, researchers and food industries have turned to innovative

* Corresponding author.
E-mail addresses: amvboas@ucp.pt (A.M. Vilas-Boas), mbrassesco@ucp.pt (M.E. Brassesco), andreiacosta94@icloud.com (A.C. Quintino), mvieira@ualg.pt (M.C. Vieira), tbrandao@ucp.pt (T.R.S. Brandão), clsilva@ucp.pt (C.L.M. Silva), miguelazevedo@decorgel.pt (M. Azevedo).

https://doi.org/10.1016/j.jfoodeng.2025.112767
Received 3 February 2025; Received in revised form 1 August 2025; Accepted 5 August 2025
Available online 8 August 2025

strategies to unlock the full potential of carob by-products and promote their economic and nutritional value.

Integral carob flour production aims to maximize the utilization of carob pods and seeds, minimizing waste and optimizing resource allocation. An essential aspect of this process is the application of milling techniques to break down the carob by-products into fine particles (Benković et al., 2017) Milling involves the use of mechanical forces to reduce the size of the materials, resulting in a more uniform and manageable product. This controlled particle size reduction enhances the accessibility of the fibers, enabling efficient valorization and the extraction of valuable components (Vilas-Boas et al., 2022) Insoluble fibers, such as cellulose and hemicellulose, can be resistant to enzymatic or microbial degradation in human gastrointestinal tract, limiting their utilization. However, through hydrolysis, these fibers can be enzymatically or chemically broken down into soluble and bioactive components (Luo et al., 2018) Enzymatic hydrolysis involves the use of specific enzymes, such as cellulases and hemicellulases, to catalyze the breakdown of complex fibers into more readily digestible forms (Ma and Mu, 2016) Chemical hydrolysis utilizes mild acids or alkaline solutions to achieve a similar effect (Loow et al., 2016). Both methods would facilitate the release of valuable nutrients and bioactive compounds from the insoluble fibers, enhancing the nutritional profile and functional properties of the resulting integral carob flour. Managing acid and alkaline residues generated from food waste processing is imperative for environmental conservation. Therefore, sustainable management practices that focus on minimizing waste generation, improving treatment efficiency, and promoting resource recovery are essential for addressing the multifaceted challenges posed by acid and alkaline residues in food waste processing. Moreover, adopting sustainable practices like waste reduction and recycling can mitigate the generation of theses residues, promoting an eco-friendlier approach to food waste processing. Regulatory oversight and continuous monitoring further ensure adherence to environmental standards, safeguarding natural resources from potential harm.

Carob syrup has traditionally been produced from carob by-products such as pulp and pods. The innovative aspect of this work lies in the insightful approach to produce carob syrup using an integrated method that valorizes whole carob flour. Additionally, no studies have been conducted on the modification of whole carob flour for use in the food industry.

In this article, we explore the concept of integral carob flour production and delve into applying an innovative milling process followed by thermal and enzymatic hydrolysis as a promising strategy for by-product valorization in the food industry. This work was part of a project in collaboration with Decorgel Produtos Alimentares S.A. We also produce and characterize a new ingredient (syrup), resultant from the carob hydrolysis, which was incorporated into a confectionery product from the company. This food product was further analyzed for digestibility, sugar and phenolic content and prebiotic and probiotic activities.

The process, benefits, and potential applications of this approach, highlighting its role in creating a more sustainable and efficient food production system, are discussed.

2. Materials and methods

2.1. Materials

Acetic Acid (CAS: 64-19-7) and Lactic Acid (CAS: 50-21-5), along with Cellulase from *Aspergillus niger*, Xylanase, 2,2′-azino-bis (3-ethylbenzothiazoline-6-sulphonic acid) (ABTS), 2,2-diphenyl-1-picrylhydrazyl (DPPH), 2,2′-azo-bis-(2-methylpropionamidine) dihydrochloride (AAPH), fluorescein disodium salt, 6-hydroxy-2,5,7,8-tetramethylchroman-2-carboxylic acid (Trolox), hydrochloric acid (HCl), sodium hydroxide (NaOH), α-amylase from porcine pancreas (A3176), pepsin from porcine gastric mucosa (P7000), pancreatin from porcine pancreas (P7545), bile bovine (B3883), D-(−)-fructose (F0127), sucrose (S4100), D-(−)-arabinose (A3131), D-(+)-mannose (M8574), D-(+)-xylose (X3877), D-glucose (G5767), and gallic acid monohydrate were procured from Sigma-Aldrich (St. Louis, MA, USA). Sulfuric Acid (CAS: 7664-93-9) was sourced from Honeywell Fluka (Buchs, Switzerland). The Folin–Ciocalteu reagent and D-galactose (CAS 59-23-4) were acquired from Merck KGaA (Darmstadt, Germany). Anhydrous sodium carbonate (Na_2CO_3) was obtained from PanReac AppliChem GmbH (Darmstadt, Germany). Methanol (≥99.9 %) was purchased from Fisher Scientific (Loughborough, UK). Ultrapure water was derived from the Milli-Q® Advantage system, Merck KGaA (Darmstadt, Germany).

2.2. Carob flour preparation

The carob pods were obtained from a regional producer in Faro, Portugal. The pods were harvested in September 2020. The integral carob flour (CF) was produced as described in Fig. 1. Whole carob pods were initially pre-grinded using a counter-rotating pin mill, followed by micronization using a cutting mill and classifier, allowing minimal dust production and fine carob flour production (this method was determined by the collaborating company and specific details are confidential).

The fine flour rest that can't be retrieved from the micronization step is considered dust. The final CF, representing >95 % of the initial carob pods, was sieved with a 45 μm mesh to obtain a fraction of flour composed mainly of insoluble fiber. This particle size was pre-established by the company as a functional size for their final product. The CF < 45 μm was collected as ingredient for the company.

The CF > 45 μm was stored and further analyzed for its nutritional and physicochemical properties before and after digestion, in order to explore this fraction for further use by the company.

2.2.1. Granulometry analysis

The particle size distribution of CF was assessed using an automatic sieve shaker (Retsch AS 200) employing circular oscillation with 50 g of flour for 5 min at an amplitude of 1.85 mm. A 20 cm diameter sieve with a mesh size of 45 μm was utilized for this analysis.

2.2.2. Carob flour nutritional analysis

All procedures followed either the guidelines outlined in the Official Methods of Analysis, the International Organization for Standardization, or the relevant Portuguese regulation (AOAC, 1990; ISO. https, 2009; ISO. https, 2013; Norma NP 518, 1986).

The crude protein content was assessed utilizing the Kjeldahl method (ISO, 20483:2013) with a conversion factor of 6.25. Lipid content was determined following AOAC method 920.39. Crude ash content was estimated through incineration (NP 518:1986). Moisture content was determined according to the ISO 24557:2009 method. Starch content was assessed using a Megazyme assay, following AOAC Method 996.11. Brix values were measured using a refractometer PR-32 (Atago®, Tokyo, Japan). All measurements were conducted in triplicate and expressed as grams per 100 g on a dry basis.

2.3. Modification process: hydrolysis optimization

The hydrolysis process was optimized considering two outcomes: small and large-scales. This modification process was considered as described by Meng-Yun Zhang. et al. (2019), Guoyong Yu. et al. (2018) and Jing Qi. et al. (2015) (Zhang et al., 2019; Yu et al., 2018; Qi et al., 2015).

For a small-scale outcome, the hydrolysis process (1:100 ratio) followed the steps represented in Fig. 2. A Box-Behnken design, a type of response surface methodology, was employed to evaluate the impact of selected factors on the solubility yield (Y) considered as the response variable (Equation (1)). This experimental design utilizes three levels for each factor within a specified range. This design allows for the estimation of first- and second-order effects, as well as interaction effects

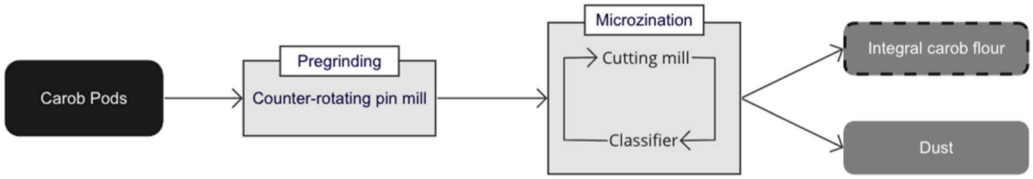

Fig. 1. Schematic representation of the milling process for the production of carob integral flour.

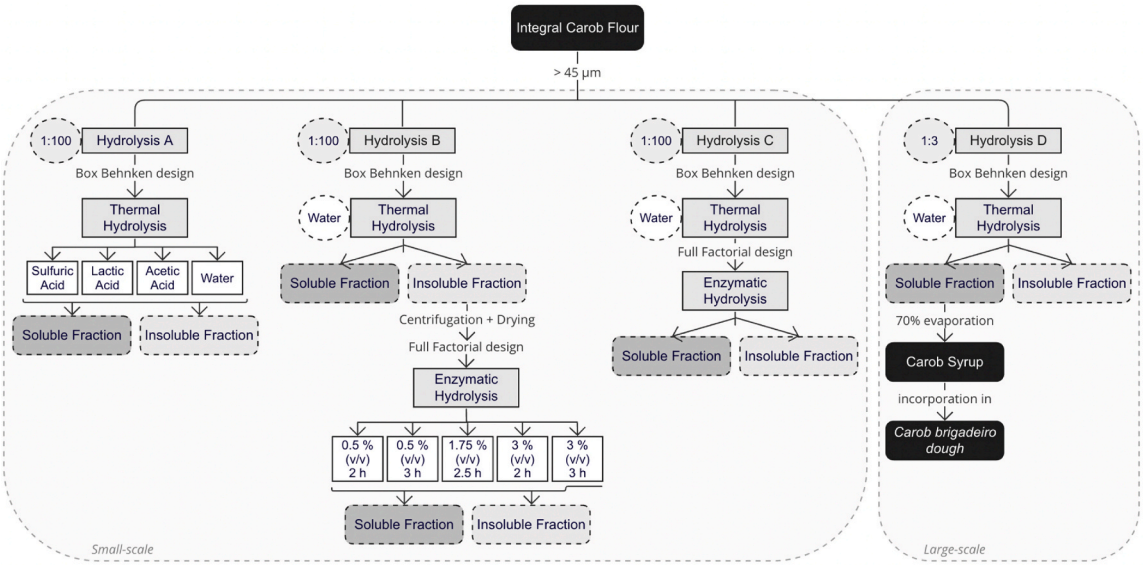

Fig. 2. Schematic representation of the hydrolysis optimization process.

between factors, while minimizing the number of required experiments.

For the *thermal hydrolysis*, the factors considered were solvent concentration (C_S) and hydrolysis time (t_{TH}). For the *enzymatic hydrolysis*, the factors evaluated were enzyme-substrate ratio (R_{ES}) and hydrolysis time (t_{EH}) (Appendix A **- Supplementary Data**).

For a *large-scale* outcome, the hydrolysis process (1:3 ratio) was minimized and followed the optimized steps represented in Fig. 2. The solubility yield was evaluated for a process comprising two consecutive steps (thermal and enzymatic) and one single step (thermal).

The three levels of the factors considered are shown in Table 1 for each hydrolysis step.

The solubility yield (Equation (1)) was calculated as the percentage ratio of hydrolysate mass (g) and initial hydrolysis CF mass (g), all in dry basis:

$$Y\ (Solubility\ Yield\ (\%)) = \frac{Hydrolysate\ mass\ (g)}{Initial\ hydrolysis\ CF\ mass\ (g)} \times 100 \qquad (1)$$

2.4. Carob syrup production

The solubilized aqueous phase resultant from the hydrolysis process was concentrated using a rotatory evaporator (Büchi® Rotavapor® R-210 evaporator, Germany), in order to produce a syrup. The solvent was evaporated until the sample reached 65–70 °Brix.

Table 1
Levels of factors considered on the hydrolysis processes design.

Factors	Low	Central point	High
		Thermal Hydrolysis	
C_S: Solvent concentration (% v/v)	0.2	1.1	2.0
t_{TH}: Hydrolysis time (min)	30	60	120
		Enzymatic Hydrolysis	
R_{ES}: Enzyme-substrate ratio	0.50	1.75	3.00
t_{EH}: Hydrolysis time (h)	2.0	2.5	3.0

2.4.1. Characterization of carob syrup

The Brix values of carob syrup (CS) samples were determined using a refractometer PR-32 (Atago®, Tokyo, Japan), with triplicate measurements conducted. CS samples underwent filtration through 0.45 µm Chromafil® PET-45/25 polyester membranes (Macherey-Nagel GmbH, Düren, Germany) and were subjected to chromatographic analysis utilizing an HPLC system comprising a WellChrom HPLC Pump K-1001, Smartline Autosampler 3800, and an RI detector K-2301 (Knauer GmbH, Berlin, Germany) for sugar profiling. Separation occurred on an Aminex HPX-87H column (BioRad, Hercules, CA, USA) at 40 °C with a mobile phase of 5 mM H_2SO_4 and a flow rate of 0.6 mL/min. Calibration curves for sucrose, fructose, and glucose were established for sugar quantification.

The thermal properties of CS were investigated using a Differential Scanning Calorimeter (DSC) 204 F1 Phoenix® (Netzsch, Bayern, Germany). Approximately 3.00 ± 0.25 mg of the analyzed sample was weighed into aluminum pans and hermetically sealed to prevent moisture loss. The CS samples were cooled to −20 °C using a refrigerated cooling system and then heated to 200 °C at a rate of 5 °C/min. An empty sealed aluminum pan served as a reference. The measurements were conducted in triplicate.

The rheological assays were monitored under steady and oscillatory modes in a HAAKE MARS III rheometer (Thermo Fisher Scientific, Karlsruhe, Germany) set with a plate–plate geometry (35 mm, 1 mm gap). A Peltier unit was used to ensure strict temperature control while a solvent trap was employed to prevent moisture absorption. The storage modulus (G′), the loss modulus (G″) and the complex viscosity (η*) were assessed by dynamic oscillatory assays performed in a frequency range of 0.01–50 Hz within the linear viscoelastic regime (the selected stress was 1 Pa). Non-linear rotational assays were performed varying the

applied shear rate from 1 s^{-1} to 200 s^{-1}. The viscoelastic parameter G′, G″ and η* were also evaluated with temperature sweep assays from 10 °C to 50 °C. The heating rate was set to 2 °C/min.

2.4.2. Confectionary application: carob brigadeiro dough

The formulation of the carob *brigadeiro* dough mixture (CBD), a carob-flavored version of the traditional Brazilian chocolate fudge, was as follows: white chocolate, glucose-fructose syrup, condensed milk, whole carob flour (10 %), hydrogenated coconut oil, emulsifiers (soy lecithin), acidity regulators (lactic acid). Further composition details are confidential.

The carob syrup by-product was introduced into the previous mixture (CBD-CS) at a concentration of 7.7 % to partially replace the glucose-fructose syrup. This food product was further analyzed for digestibility, sugar and phenolic content and prebiotic activity.

2.4.2.1. Simulated gastrointestinal tract digestion. The dough of carob *brigadeiro* with (CBD-CS) and without carob syrup (CBD) underwent a modified INFOGEST protocol, from which duplicate aliquoted samples were collected at each phase of the gastrointestinal tract (GIT) for subsequent analysis (Brodkorb et al., 2019).

In the oral phase, CBD-CS was mixed with pre-warmed simulated salivary fluid (SSF) to achieve a paste-like consistency. α-Amylase, prepared in water at a concentration of 75 U/mL, was added to the mixture, which was then incubated for 2 min at 37 °C with agitation at 180 rpm. Duplicate aliquoted samples were obtained.

For the gastric phase, pre-warmed simulated gastric fluid (SGF) was added to the previous samples at a 1:1 (v/v) ratio. Pepsin, prepared in water at a concentration of 2000 U/mL, was added, and the pH was adjusted to 3. The mixtures were incubated for 2 h at 37 °C with agitation at 120 rpm. Due to the low lipid content, gastric lipase was not added. Duplicate aliquoted samples were collected.

In the intestinal phase, pre-warmed simulated intestinal fluid (SIF) was added to the previous samples at a 1:1 (v/v) ratio. Pancreatin and bile, prepared in SIF at concentrations of 100 U/mL and 10 mM, respectively, were added to the digesta, and the pH was adjusted to 7. The mixtures were incubated for 2 h at 37 °C with agitation at 60 rpm.

The intestinal samples underwent simulated dialysis using two methods: a) overnight dialysis with a membrane pore size of 3.5 kDa at 37 °C and 60 rpm; b) Caco-2/HT29-MTX Transwell® cells. Retained samples were collected, and absorbed samples were freeze-dried for further analysis.

Finally, the retained aliquoted samples from the oral, gastric, and intestinal phases were centrifuged and filtered through 0.45 μm Chromafil® PET-45/25 polyester membranes (Macherey-Nagel GmbH, Düren, Germany) to remove digestive enzymes.

2.4.2.1.1. Sugar content. The digested samples of CBD and CBD-CS were passed through 0.45 μm Chromafil® PET-45/25 polyester membranes (Macherey-Nagel GmbH, Düren, Germany) and subjected to chromatographic analysis using an HPLC system comprising a WellChrom HPLC Pump K-1001, Smartline Autosampler 3800, and an RI detector K-2301 (Knauer GmbH, Berlin, Germany). Separation was carried out on an Aminex HPX-87H column (BioRad, Hercules, CA, USA) maintained at 40 °C, with a mobile phase consisting of 5 mM H_2SO_4 and a flow rate of 0.6 mL/min. Calibration curves were established for the quantification of sucrose, fructose, and glucose. The Suqec index was measured according to Brassesco et al. (2023) (Brassesco et al., 2023).

2.4.2.1.2. Total phenolic content. The total phenolic content (TPC) of the digested CBD and CBD-CS samples was determined using a modified Folin–Ciocalteu colorimetric method, following the procedure outlined by Coscueta et al. (2018) In a 96-well microplate, 30 μL of the sample (diluted in methanol) was combined with 100 μL of Folin–Ciocalteu reagent (20 % v/v) and 100 μL of anhydrous sodium carbonate solution (7.4 % w/v), in that order. Methanol was used as the control. A standard curve was generated using concentrations ranging from 0.025 to 0.2 mg/mL of gallic acid. The microplate was then incubated at 25 °C for 30 min, and the absorbance of the resulting blue mixtures was measured at 765 nm using a Multidetection plate reader (Synergy H1, Agilent, Santa Clara, Utah, USA). Duplicate measurements were performed for each phase of the gastrointestinal tract (GIT). TPC values were expressed in milligrams of gallic acid equivalents (GAE) per milliliter of sample.

2.4.2.1.3. Antioxidant activity. The overall antioxidant activity of the digested CBD and CBD-CS samples was assessed using a modified ABTS method, following the protocol outlined by Gonçalves et al. (2009) (Gonçalves et al., 2009). ABTS was dissolved in water to achieve a concentration of 7 mM. The ABTS radical cation (ABTS•+) was generated by mixing the ABTS stock solution with potassium persulfate (Merck) to reach a final concentration of 2.44 mM and allowing it to stand in the dark at room temperature (25 ± 2 °C) for 12–16 h before use. Prior to analysis, the ABTS•+ solution was filtered using a 0.22 μm filter (Orange Scientific, Braine-l'Alleud, Belgium) and diluted in methanol to achieve an absorbance of 0.700 ± 0.020 at 734 nm. In a 96-well microplate, 20 μL of the sample was mixed with 180 μL of the ABTS•+ working solution. Methanol was utilized as the control. A standard curve was established using concentrations ranging from 25 to 175 μM of Trolox. The microplate was then incubated at 30 °C for 5 min, and the absorbance of the resulting mixtures was measured at 734 nm using a Multidetection plate reader (Synergy H1, Agilent, Santa Clara, Utah, USA). Duplicate measurements were conducted for each phase of the gastrointestinal tract (GIT), and the results were expressed in μmol of Trolox equivalents per mL of sample.

The overall antioxidant activity of the digested CBD and CBD-CS samples was determined using a modified DPPH method, following the procedure described by Brand-Williams et al. (1995) (Brand-Williams et al., 1995) DPPH was dissolved in methanol to achieve a concentration of 600 μM. Prior to analysis, DPPH• was diluted in methanol to achieve an absorbance of 0.600 ± 0.100 at 515 nm. In a 96-well microplate, 25 μL of the sample was mixed with 175 μL of the DPPH• working solution. Methanol served as the control. A standard curve was established using concentrations ranging from 25 to 250 μM of Trolox. The microplate was then incubated at 25 °C for 30 min, and the absorbance of the resulting mixtures was measured at 515 nm using a Multidetection plate reader (Synergy H1, Agilent, Santa Clara, Utah, USA). Duplicate measurements were conducted for each GIT phase, and the results were expressed in μmol of Trolox equivalents per mL of sample.

2.4.2.1.4. Prebiotic and probiotic activities

2.4.2.1.4.1. Prebiotic activity

Bifidobacterium animalis B_0, *Bifidobacterium animalis* subsp. *lactis* Bb12, *Bifidobacterium longum* subsp. *longum* BG3, *Lacticaseibacillus casei* 01, *Lacticaseibacillus rhamnosus* R11 and *Lactobacillus acidophilus* Ki were employed to assess the prebiotic potential of the carob-products produced in this study (CF, CS, CBD and CBD-CS). All bacterial strains were stored at −80 °C in MRS broth (Biokar Diagnostics, Beauvais, France) supplemented with 30 % (v/v) glycerol.

For L. *casei* 01, *L. rhamnosus* R11 and *L. acidophilus* Ki, bacterial colonies were suspended in MRS broth to achieve a turbidity of 0.5 McFarland and subsequently diluted to obtain a final concentration of 5 × 10^5 CFU/mL. A volume of 20 μL of the inoculum was dispensed into a 96-well microplate, and CF, CS, CBD and CBD-CS samples, diluted in basal MRS broth without glucose, were added at concentrations of 1 % (v/v). The plates were then incubated at 37 °C with agitation for 26 h using a Multiskan GO microplate reader (Thermo Scientific, Waltham, MA, USA).

For *B. animalis* B_0, *B. lactis* Bb12 and *B. longum* BG3, inocula were prepared under anaerobic conditions by suspending bacterial colonies in MRS broth supplemented with 0.05 % (v/v) L-cysteine-HCl, adjusting the suspension to a turbidity of 0.5 McFarland, and diluting to reach a final concentration of 5 × 10^5 CFU/mL. Similarly, 20 μL of the inoculum was added to a 96-well microplate along with CF, CS, CBD and CBD-CS samples diluted in basal MRS broth without glucose at 1 % (v/v). The

microplates were sealed with parafilm and incubated at 37 °C with agitation for 48 h.

In both experimental setups, optical density (OD) measurements were recorded every hour at 620 nm. The negative control consisted of basal MRS broth alone, while the positive controls were MRS broth supplemented with glucose and fructooligosaccharides (FOS).

2.4.2.1.4.2. Cell lines

Human Caucasian colon carcinoma epithelial cells (Caco-2, ECACC 86010202) and HT29-MTX E12 (ECACC 12040401) were obtained from the European Collection of Authenticated Cell Cultures. They were cultured in DMEM (Gibco, Thermo Scientific, USA) supplemented with 10 % (v/v) FBS from Biowest (France) and 1 % (v/v) of Penicillin-Streptomycin-Fungizone (Lonza, Switzerland). Additionally, the media were supplemented with 1 % (v/v) non-essential amino acids (Gibco, Thermo Scientific, USA). Both cell lines were maintained at 37 °C in a humidified atmosphere containing 5 % CO_2 and 95 % air.

2.4.2.1.4.3. Co-culture models

The co-culture models were established following the methods outlined by Antunes et al. (2013) with adaptations (Antunes et al., 2013) In summary, Caco-2/HT29-MTX co-cultures were seeded onto the apical chamber of a 12-well Transwell® plate (Corning, New York, USA) at a ratio of 90:10, respectively, to achieve a monolayer with a final density of 1×10^5 cells/cm^2 in each insert. These co-cultures were then maintained for 21 days prior to experimentation.

2.4.2.1.4.4. TEER measurements

The integrity of the membranes in the various models was assessed by measuring transepithelial electrical resistance (TEER) using a Millicell® ERS-2 Voltohmmeter (Merck, Germany) with the digested CBD and CBD-CS samples. It's important to highlight that only monolayers exhibiting TEER values ranging from 150 to 250 Ω/cm^2 were chosen for permeability experiments.

2.4.2.1.4.5. Permeability measurements

The permeability of the digested CBD and CBD-CS samples was assessed by modifying the techniques outlined by Antunes et al. (2013) (Antunes et al., 2013). In summary, the media in the apical chamber of the 21-day differentiated Caco-2/HT29-MTX co-culture were replaced with either plain media (basal control), media containing digested samples, or media with 10 % (v/v) DMSO (stress control). The plate was then re-incubated for 3 h.

2.4.2.1.4.6. Glucose content

The samples obtained from the TEER assay were evaluated for glucose content using the same method described in section 2.4.2.1.1.

2.5. Statistical analysis

Statistical analysis was performed using GraphPad Prism, v. 8.4.0 software (GraphPad Software, San Diego, CA, USA). Both normality and homoscedasticity assumptions were met; hence, analysis of variance (two-way ANOVA), with a 95 % confidence level, was applied to every dependent parameter, to assess differences between the different samples. Tukey's test was used for means' multiple comparisons. In all tests performed, the significance level was set to 5 %. The multiple t-tests were performed with a predetermined significance level (e.g., a = 0.05) to determine statistical significance. The results of the multiple t-tests provided insights into specific group differences, contributing to a deeper understanding of the data and the factors influencing the outcome variable.

The Box-Behnken design, as a response surface methodology, enables the construction of a model that incorporates linear, quadratic, and interaction effects of the independent factors under study on the solubility yield.

For the thermal hydrolysis, the model is:

$$Y = \beta_0 + \beta_1 C_S + \beta_2 t_{TH} + \beta_3 C_S^2 + \beta_4 C_S t_{TH} + \beta_5 t_{TH}^2 \quad (2)$$

and for the enzymatic hydrolysis, the model is:

$$Y = \beta_0 + \beta_6 R_{ES} + \beta_7 t_{EH} + \beta_8 R_{ES}^2 + \beta_9 R_{ES} t_{EH} + \beta_{10} t_{EH}^2 \quad (3)$$

Where β_i (i = 0 to 10) denotes the model coefficients obtained by multiple regression analysis (Coscueta et al., 2018, 2021; Gunst, 1996) An analysis of variance (ANOVA) was used to assess the significance of each coefficient, as shown in Appendix A (**Supplementary Data**).

Models, excluding non-significant terms, were developed. The coefficient of determination (R^2) was calculated for each model to assess the proportion of variance in the dependent variable that can be explained by the independent variable(s) included in the models.

The response surface methodology also allows for the optimization of responses, as a maximum of the regression models can be obtained. Surface plots were generated to visually interpret the impact of the factors. Optimization of responses was performed using the Derringer desirability function to achieve the best solubility yield, with desirability values ranging between 0 and 1. Data analysis was executed in Minitab® 17.1.0, ensuring robust statistical evaluations (Derringer and Suich, 1980).

3. Results and discussion

3.1. Carob flour characterization

The produced CF was characterized by its proximate composition (Table 2). The results revealed a high content of total carbohydrates and relatively low solubility, as expected in carob-based products known for their high fiber content. These results are in accordance with previously produced carob flours, which indicate that the milling process used for processing the carob pods is adequate to produce a functional CF that has not undertaken a roasting process (Vilas-Boas et al., 2022; Brassesco et al., 2023) Roasting is the most common processing method for obtaining commercial carob flours (Brassesco et al., 2021; Özcan et al., 2007).

The CF was separated into size fractions to obtain a fraction with particle sizes >45 μm, which may pose some challenges when incorporated as an ingredient in pastry and bakery products formulations within the food industry. The particle size distribution, revealed that, in comparison to other processing methods, a smaller fraction of particles >45 μm was achieved. This indicates that the methodology employed in this study allowed to produce a finer CF, with over 65 % of the particles being ≤45 μm.

The fraction ≤45 μm was considered optimal as the final CF product and collected by the company, whereas the >45 μm fraction is presumed to be richer in insoluble fiber and, consequently, more challenging to incorporate into food formulations. This >45 μm CF fraction was selected for further analysis and processing towards syrup (using hydrolysis methodologies).

3.2. Optimization of modification processes

The obtained CF > 45 μm was subject to a hydrolysis process, aiming to further solubilize and modify the CF to obtain valuable by-products. These by-products are of interest for incorporation into food

Table 2
Proximate composition of carob flour.

Proximate Composition (g/100 g Dry Basis)	Carob Flour
Moisture	7.91 ± 0.07
Ash	2.48 ± 0.05
Carbohydrate	83.70 ± 0.14
Protein	5.59 ± 0.23
Lipids	0.33 ± 0.01
Total Starch	1.05 ± 0.18
Solubility (25 °C)	43.16 ± 0.97
Solubility (90 °C)	36.35 ± 0.57
°Brix (20 °C)	60.80 ± 0.00

formulations, contributing to the valorization of the carob-products production chain.

The hydrolysis optimization started by considering a small-scale setting. Firstly (Hydrolysis A), the CF was solubilized in aqueous solvent in a ratio of 1:100. Using a Box Behnken design, the thermal hydrolysis was tested and validated for different solvents at different concentrations and for different run periods at 100 °C. The solvents chosen were sulfuric acid, lactic acid, acetic acid and a control (deionized water) at 0.2, 1.1 and 2 % (v/v), for 30, 60 and 120 min (Qi et al., 2015) It is important to note that sulfuric acid is not suitable for food-grade applications; however, it was selected as a positive control due to its excellent hydrolysis capacity.

The results obtained for the solubility yield (%) suggested that the most suitable solvent tested was acetic acid at 1.02 % (v/v) for 120 min, with an experimental solubility yield of 56.07 ± 0.58 % (Table 3). When comparing the acetic acid against the control of deionized water (solubility yield of 55.84 ± 0.84 %), the difference in solubility yield was not significant. This finding supports the selection of water as the solvent for the thermal hydrolysis step, given its greener and more sustainable profile.

The next step in optimizing hydrolysis involved evaluating the enzymatic hydrolysis step. In this phase, the CF underwent thermal hydrolysis under previously optimized conditions. Subsequently the remaining insoluble fraction was subjected to centrifugation (10768 g for 15 min), followed by drying (O.N. at 60 °C) and, then submitted to enzymatic hydrolysis (Hydrolysis B). Using a full factorial design, the enzymatic hydrolysis, utilizing a mixture of xylanase (48 U/g) and cellulase (90 U/g), was systematically tested and validated for various enzyme/substrate ratios and run periods at a 55 °C temperature and pH 5 (R^2 = 0.7270 and desirability of 0.76) (Zhang et al., 2019; Yu et al., 2018).

The results showed that lower enzyme/substrate ratios and shorter run period led to higher experimental solubility yield (Table 4). This observation could be attributed to the enzymes reaching maximum activity and saturation under these conditions.

When combining the solubility yields from hydrolysis A and B, the process achieved an approximately 80 % solubility yield. This was accomplished by incorporating a thermal hydrolysis step followed by an enzymatic hydrolysis step applied to the initially obtained insoluble fraction. To optimize this modification and solubilization process further, the next approach compared the results with a similar process employing a continuous course. In this continuous approach, after the thermal hydrolysis step, the remaining fraction was not separated and dried but instead underwent continuous enzymatic hydrolysis after the thermal step, aiming to minimize process steps and overall cost.

Hydrolysis C (continuous process) was tested and validated under the same conditions optimized in the previous hydrolysis A and B. However, the results indicated that only a ~50 % solubility yield was achieved (Table 5). Although enzymatic hydrolysis (Hydrolysis C) was applied immediately after thermal hydrolysis, the retained soluble fraction may have substantially increased the viscosity of the mixture. Higher viscosity can impair mass transfer and enzyme diffusion, particularly during the early stages of hydrolysis, leading to reduced reaction rates and diminished enzymatic efficiency (Da Silva et al., 2020). Therefore, it is plausible that the presence of a viscous soluble phase contributed to the observed minimal effect of enzyme application on the insoluble fraction, ultimately limiting the overall hydrolytic conversion capacity. Furthermore the fiber structure within the matrix, which may undergo modification when the matrix is dried, may allow the enzymes mixture to take action, as observed in the case of Hydrolysis B vs Hydrolysis C.

Table 4
Results for Hydrolysis B obtained for the response surface regression experiment.

Parameters	Hydrolysis B
Optimal E/S % (v/v)	0.5
Optimal Run Period (h)	2
R^2	0.7220
Desirability	0.76
Theoretical Solubility Yield (%)	23.45
Experimental Solubility Yield (%)	23.46 ± 1.73

Table 5
Solubility yield results for Hydrolysis B vs Hydrolysis C vs Hydrolysis D.

Solvent	Experimental Solubility Yield (%)
Hydrolysis B (fractioned process and small-scale)	
Deionized Water	Total of ~79
Hydrolysis C (continuous process and small-scale)	
Deionized Water	51.73 ± 3.40
Hydrolysis D (large-scale)	
Deionized Water	50.48 ± 0.83

When evaluating the conditions for each hydrolysis, the choice of the process to pursue was based on factors such as environmental impact, cost, and simplicity. Consequently, Hydrolysis A, under optimal conditions, emerged as the selected methodology, yielding approximately 50 % solubility and generating two by-products (soluble and insoluble by-products) from the initial CF > 45 μm. The subsequent phase involved scaling up this process for large-scale application (Hydrolysis D). The chosen conditions were applied with an initial CF:Water ratio of 1:3, as this represented the minimum ratio that allowed the CF to achieve a paste-like consistency when mixed with deionized water and this lower ratio is more applicable and suitable at industrial level. The resultant by-products obtained for the optimized thermal hydrolysis were a soluble fraction and an insoluble fraction. Regarding the experimental solubility yield, no significant differences were observed when varying the initial CF:Water ratio (Table 5).

Moreover, sugar content was assessed for all tested hydrolyses (A to D), as presented in Table 6. The results indicated that the samples obtained for the enzymatic hydrolysis step (Hydrolyses B) had the lowest sugar content, confirming that this step had minimal influence on the resultant fractions. Furthermore, the optimization of the hydrolysis process and solubility yield led to an increase of the % Suceq and simple sugars, as showed for Hydrolysis D. This resulted in a more appealing by-product rich in sugars, potentially suitable for further processing into a syrup, for example.

For this work, the soluble fraction by-product from the best hydrolysis (D) was further processed, studied and incorporated as an ingredient in food formulations.

3.3. Carob syrup production and characterization

The soluble by-product obtained from Hydrolysis D underwent

Table 3
Solubility yield results for Hydrolysis A, testing sulfuric acid, lactic acid, acetic acid and deionized water for the surface response regression experiment.

	Hydrolysis A					
Solvent	Optimal Run Period (min)	Optimal Concentration %(v/v)	Theoretical Solubility Yield (%)	Desirability	R^2	Experimental Solubility Yield (%)
Sulfuric Acid	75	0.20	60.60	0.77	0.5963	58.58 ± 0.65
Lactic Acid	120	0.20	54.14	0.80	0.7261	56.27 ± 0.87
Acetic Acid	120	1.02	54.79	0.90	0.8902	56.07 ± 0.58

Table 6
Sugar content obtained throughout the optimization of the hydrolysis process of CF > 45 μm.

	Parameter	% Sucrose/Sample	% Glucose/Sample	% Fructose/Sample	% Suceq
Hydrolysis A	Sulfuric Acid	2.90 ± 0.50	0.09 ± 0.02	6.20 ± 0.67	13.68
	Lactic Acid	0.59 ± 0.08	1.30 ± 0.69	1.69 ± 0.74	4.48
	Water	0.26 ± 0.02	0.59 ± 0.02	0.50 ± 0.06	1.55
Hydrolysis B (E/S % (v/v))	0.5 % for 2 h	–	0.80 ± 0.17	0.57 ± 0.16	1.58
Hydrolysis C	Water	13.35 ± 1.95	16.39 ± 0.66	12.30 ± 1.78	46.75
Hydrolysis D	Water	34.10 ± 3.46	8.91 ± 0.91	6.50 ± 0.68	52.83

analysis for dissolved solids to estimate the total sugars present. As indicated by the results, the °Brix of the directly obtained juice was below the standard range of 65–70 %. To address this, the soluble by-product (°Brix of around 20 %) was evaporated to reduce its volume by 70 %, resulting in an increased °Brix of approximately 72 %. This process facilitated the production of Carob Syrup (CS) as a by-product of the hydrolysis.

The sugar content of the CS was analyzed, and the main sugar identified was sucrose, with a concentration of 34.10 ± 3.46 g/100 g dry basis (DB). Glucose and fructose were also detected at lower levels, with contents of 8.91 ± 0.91 g/100 g DB and 6.50 ± 0.68 g/100 g DB, respectively. The total sugar equivalent (Suceq) was calculated as 52.83 g/100 g DB. Additionally, the °Brix value of the syrup was determined to be 71.50 ± 2.85, indicating a high soluble solids content typical of concentrated syrups. These results are in accordance with other carob syrups reported in the literature. Edwards et al. (2016) and Papaefstathiou et al. (2018) characterized and studied carob syrup as a sweetener and similar results were obtained for the quantification of sucrose, fructose and glucose in sugar content (Papaefstathiou et al., 2018; Edwards et al., 2016).

The CS was further analyzed in terms of behaviour under standard cooking temperatures. The results showed that the product exhibits a melting temperature (T_m) of approximately 130 °C, which has been previously reported for carob-based products such as CF with different moisture content and particles from carob waste (Fig. A1) (Saitta et al., 2023; Infurna et al., 2022) This thermal transition point is characteristic of fructose thermal transition, one of the sugars present in the analyzed CS (Wang et al., 2019; Lee et al., 2011).

Fig. 3 shows that carob syrup is considered a viscous gel, since G'' (loss modulus) was greater than G' (storage modulus) over the entire frequency range (Rahman et al., 2020).

As the frequency increased, the phenomenon of "crossover", i.e. the intersection between the two moduli, was not observed. A crossover point occurs when the elastic and viscous behaviors are equally weighted ($G' = G''$) (Erturk et al., 2023).

The absence of a crossover point indicates that the syrup exhibits predominantly viscous behavior under the tested conditions, with minimal elastic (solid-like) response. The lack of such a transition in carob syrup suggests that its molecular structure does not form a stable network, and it behaves more like a concentrated viscous solution rather than a structured gel.

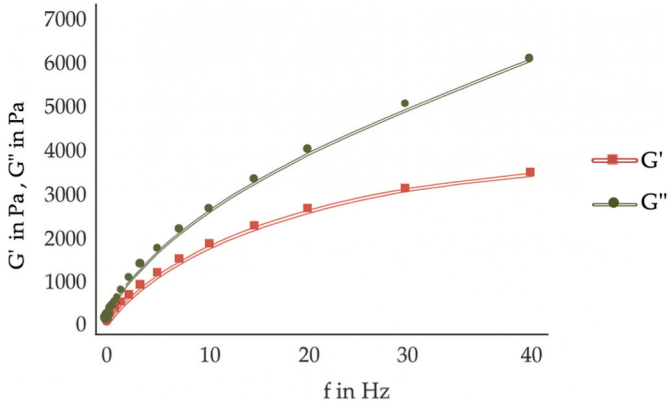

Fig. 3. – Storage modulus G′ and loss modulus G″ as a function of carob syrup frequency (f).

3.4. *By-product application: carob brigadeiro dough (CBD) digestibility evaluation*

The CS was incorporated into a carob *brigadeiro* dough (CBD-CS) as a substitute for glucose-fructose syrup, a common sweetener in the food industry. The digestibility of this food matrix was evaluated through a simulated gastrointestinal setting (INFOGEST), comparing sugar content, total phenolic content (TPC), antioxidant activity (AA) and bioaccessibility with the normal formulation of the carob *bridageiro* dough (CBD).

The sugar content showed that sucrose was the sugar in higher quantity throughout the GIT digestion (Fig. 4). The gastric and intestinal phases promote the increase in glucose and fructose content, which can be due to the enzymatic cleavage and degradation of glycoside bonds, by extreme conditions such as acidity, and the inversion of sucrose into glucose and fructose units (Vilas-Boas et al., 2022; Gunel et al., 2020). There was a noticeable increase in sucrose content, in the intestinal phase, possibly due to the presence of other and more complex sugars, as described in literature, which are broken into sucrose molecules, detected by the HPLC method used (Nasar-abbas et al., 2016).

AA and TPC increased after the gastric and intestinal phases (Fig. 5), as gastric and intestinal digestive enzymes and bile salts may act on the food matrix, indicating the release of these phenolic compounds from the phenolic–protein conjugates or the increase of the reactivity of phenolic compounds towards the Folin–Ciocalteu reagent (Chait et al., 2020; Zhu et al., 2019; Wootton-Beard et al., 2011). The higher AA showed for CBD-CS can be attributed to the high content of TPC in CS, as described in literature, or to the other antioxidant compounds like peptides, organic acids and products of non-enzymatic browning and Maillard reactions naturally produced during thermal hydrolysis of the integral carob flour (Rodríguez-Solana et al., 2021).

These results suggest that the rupture of high-molecular complexes of the *brigadeiro* matrix and partial deterioration of phenolics leads to the production of different types of antioxidant compounds, as well as pH changes could promote the deprotonation of hydroxyl groups present on the phenolic aromatic rings (Chait et al., 2020; Baker et al., 2013; Martínez-Las Heras et al., 2017). Previous studies on integral carob flour showed an increase of AA and TPC on the gastric phase, as observed for CBD and CBD-CS samples. By contrast, the food matrices tested in this work display a further increase of AA and TPC throughout the rest of GIT digestion (Vilas-Boas et al., 2022). Other studies on carob extracts, showed similar TPC and AA profiles to those obtained for this work, throughout the GIT (Ydjedd et al., 2017) Studies on carob pasta and carob liqueurs, showed an increase in TPC and AA values after GIT digestion (Goulas and Hadjisolomou, 2019; Jakobek, 2015; Rodríguez-Solana et al., 2019).

Furthermore, the digested CBD and CBD-CS was analyzed for its prebiotic activity and permeability at the intestinal phase.

The results for the prebiotic activity of these matrixes on six different bacterial strains are presented in Fig. 6. CS and CF samples exhibited

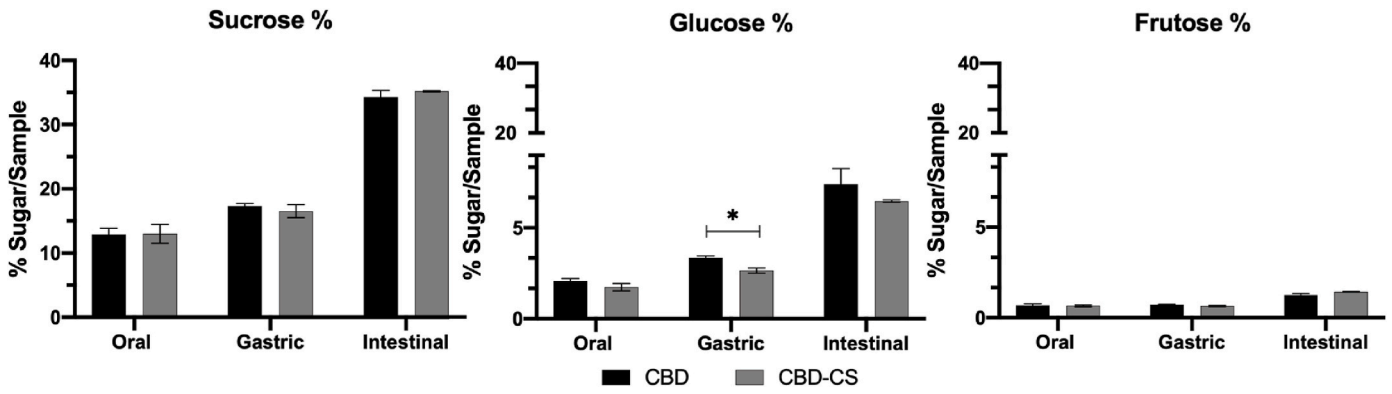

Fig. 4. Sucrose, glucose and fructose content in CBD and CBD-CS throughout GIT simulation. The bars represent the standard deviation.

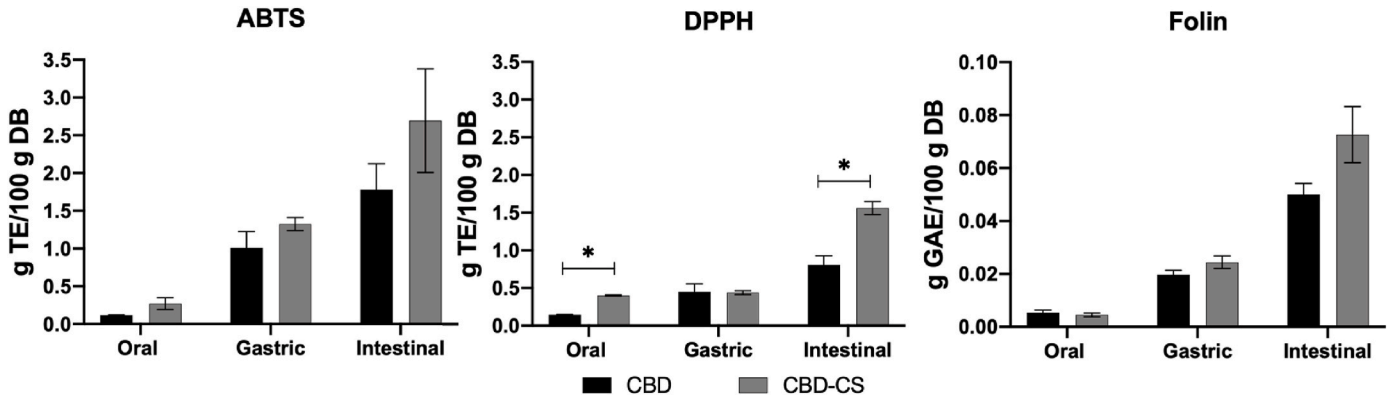

Fig. 5. Antioxidant capacity (ABTS and DPPH assays) and Total phenolic compounds (Folin–Ciocalteu method) of CBD and CBD-CS in the simulated GIT. All results expressed in g/100 g on dry basis (DB). The bars represent the standard deviation. Asteriks represent significant difference between samples.

prebiotic activity for most tested bacterial strains (*L. casei* 01, *B. animalis* B_0, *L. rhamnosus* R11 and *B. animalis* Bb12). On the other hand, results showed that the CS and CF lose their prebiotic capacity once incorporated into the *brigadeiro* matrix, for all tested strains. These results are not in accordance with the sugar content determination (Fig. 4), where the sugars increase as the digestion progresses. This can be possible as prebiotic activity is not linear and can be influenced by various factors, such as the presence of molecules that counter the prebiotic activity, like polyphenols and organic acids, that may act as antimicrobial agents (Gómez-García et al., 2022).

Previous studies on carob-supplemented products showed an initial prebiotic activity on *Lactobacillus rhamnosus* (Mahtout et al., 2016) In contrast, studies made with roasted carob flour, results showed a decrease in prebiotic activity due to the presence of Maillard products, which exhibited bactericidal properties (Polanowska et al., 2021).

Lastly, the digested intestinal CBD and CBD-CS samples were analyzed for their cytotoxicity and permeability on Caco-2/HT26-MTX co-culture. The results are shown in Fig. 7. This co-culture was used as a permeability reference for mimicking the gap-junctions of intestinal epithelial cells, responsible for absorbing nutrients in the intestine and produce mucus, which plays an important role in the absorption of nutrients for the bloodstream.

The cytotoxicity results showed that the maximum concentration of sample that does not inhibit cellular growth was 0.5 % (w/v) of CBD and CBD-CS (Fig. 7a). Samples at 1 % (w/v) were toxic for this co-culture, supporting the selection of 0.5 % (w/v) as the concentration to test for *in vitro* permeability. A study on the carob syrup cytotoxic effect on SH-5YSY, 3T3 and D3 cell lines showed inhibitory concentrations (IC_{50}) ranging from 100 to 500 μg/mL but no toxic effect on non-cancerous cells, proving a potential for selectivity to cancer cell lines apoptosis. Hydrophobic and low molecular weight compounds, such as polyphenols, present in carob syrup could permeate through the cellular membrane causing loss of cell integrity and cell death (Dhaouadi et al., 2014).

As for the *in vitro* permeability determination, the results showed that after 2 h of test, approximately 20 % of membrane recovery was reached, which is close to the values obtained for the stress control (Fig. 7b). This implied that, after 2 h, the cellular membrane burst, due to the glucose content permeated that increased over the tested time, for both samples. Additionally, there was an increase in glucose content for the apical samples, given that the membrane burst promoted the spread of glucose throughout the plate-well.

Previous studies on carob-based products showed cytotoxic effects of these products on cancer cellular lines (HeLa, HCT-116, DU-145, HEp-2, HT-29 and PLHC-1) after 24 h of incubation (Ben Othmen et al., 2020; Custódio et al., 2011; Nagib et al., 2010; Ghanemi et al., 2017) Studies on carob seed peel and pod extracts showed a significant reduction of cell viability for 0.5 mg/mL of sample in RAW 264.7 cells (Rico et al., 2019).

The results obtained demonstrate the high potential of this hydrolysis methodology for the obtention of an added-value food ingredient that presents a vast desirable profile in today's consumer demands. Industrial-scale implementation of carob syrup production through thermal hydrolysis of carob flour, using the determined optimal conditions tested in this study, presents a few practical limitations. These may include the energy requirements for heating and evaporation, handling of large volumes of water, and the need for equipment capable of managing high-fiber biomass. Furthermore, process scalability must ensure consistent extraction efficiency and syrup quality, while minimizing operational costs. Nonetheless, adopting this approach aligns

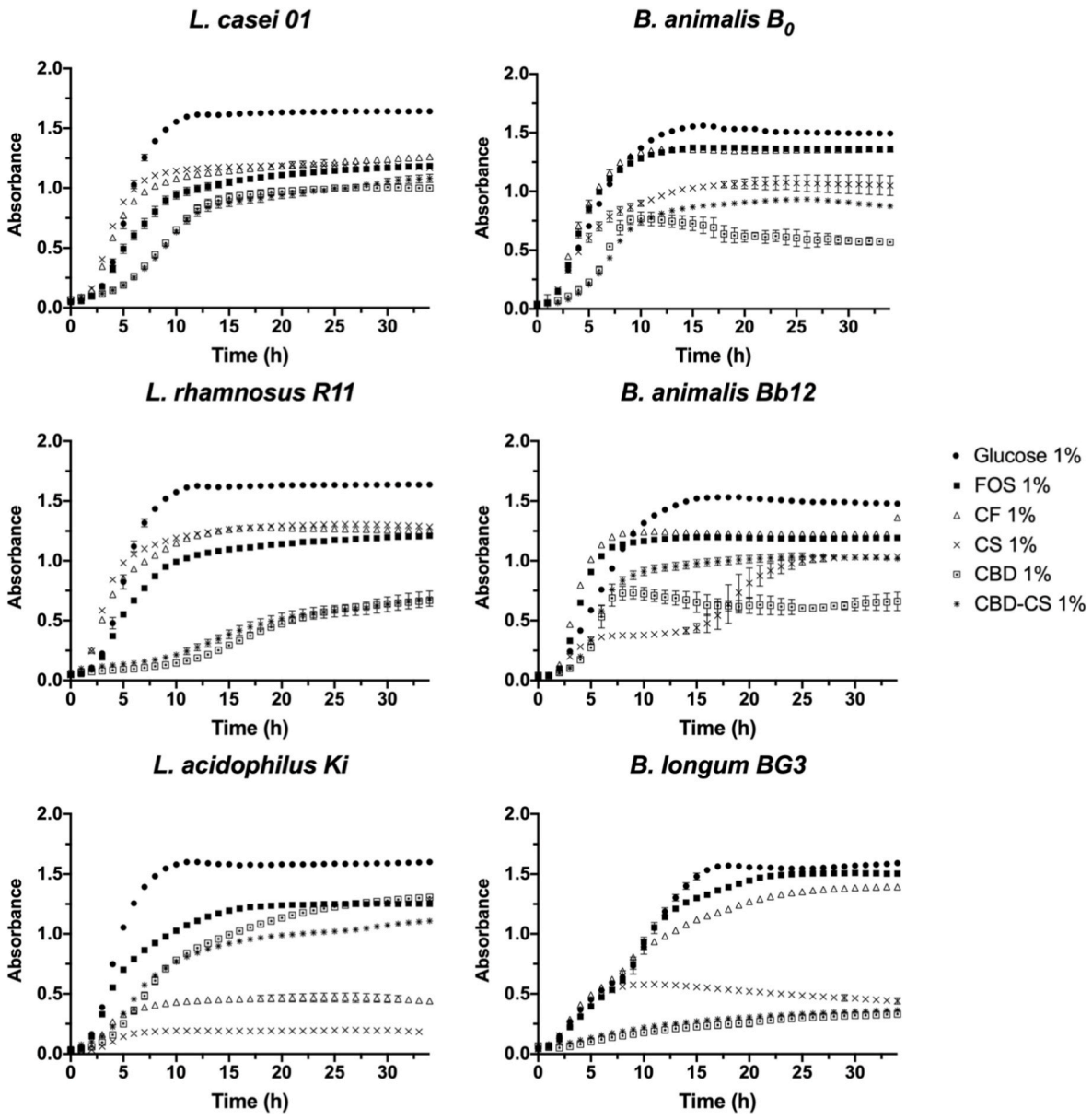

Fig. 6. Prebiotic activity of CBD and CBD-CS on Lactobacillus and Bifidobacterium strains, after intestinal digestion. The bars represent the standard deviation.

strongly with zero-waste principles, allowing for the valorization of carob by-products into high-value ingredients. It is important to note that this study did not assess the tannin content of the carob syrup, which may be relevant given the potential co-extraction of condensed tannins during thermal hydrolysis. As these compounds can influence the sensory properties of the final product, particularly in terms of bitterness and astringency, future work should include both tannin quantification and structured sensory evaluation to more comprehensively assess the quality and consumer acceptance of thermally processed carob syrup.

Finally, carob syrup, naturally rich in antioxidants, dietary fiber, and with a favorable sugar profile and low glycemic index, offers both nutritional and environmental benefits. As consumers increasingly seek sustainable and health-focused alternatives, investing in such processes contributes to circular economy goals while creating marketable, added-value food solutions.

4. Conclusions

The present study demonstrates a novel and sustainable approach to the valorization of carob by-products through the development of carob syrup from modified integral carob flour. By employing an optimized thermal hydrolysis process using only water at a 1:3 solid-to-liquid ratio, the method aligns with clean-label and environmentally friendly production principles, offering a low-cost and scalable solution that avoids the use of chemical agents or harsh processing conditions. The resulting syrup exhibited a high antioxidant capacity, enriched total phenolic content, and a balanced sugar composition, confirming its potential as a functional ingredient suitable for use as a prebiotic agent or a natural alternative to conventional sweeteners.

The innovation aspect of this study resides in the full utilization of integral whole carob flour maximizing the use of available biomass while minimizing residual waste. The nutritional value of the syrup, characterized by the presence of dietary fiber, bioactive phytochemicals such as polyphenols, and a low glycemic index, further enhances its suitability for incorporation into health-focused food products aimed at

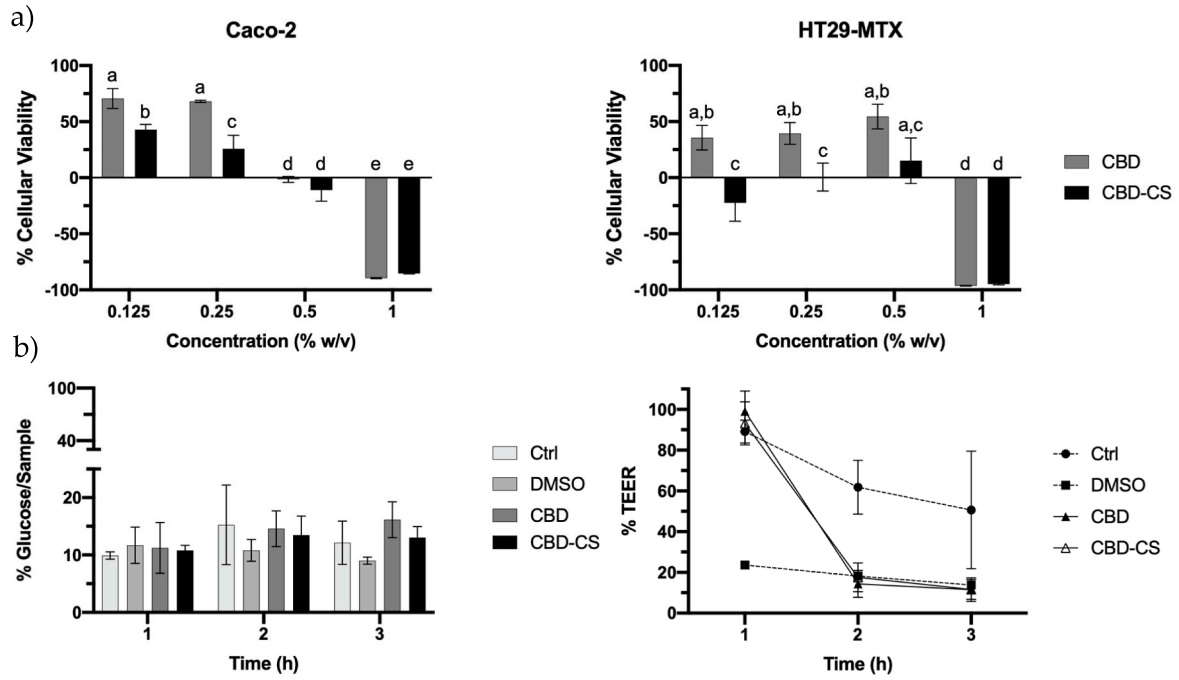

Fig. 7. (a) Cellular viability (%) determination for CBD and CBD-CS intestinal digested samples, after 3 h of assay. The bars represent the standard deviation. Letters represent significant difference between samples. (b) In vitro permeability determination for %Glucose/sample over a 3 h assay on basal samples; % TEER over a 3 h assay on basal samples. Ctrl – basal control; DMSO – stress control. The bars represent the standard deviation. Asteriks represent significant difference between samples.

consumers seeking alternatives to refined sugars and artificial additives.

This approach not only contributes to waste reduction but also embodies a circular economy model within agri-food systems, turning what would typically be considered a low-value by-product into a high-value multifunctional food ingredient. By bridging technological feasibility with nutritional and environmental relevance, this study underscores the importance of investing in zero-waste strategies and the development of added-value ingredients that meet both sustainability and consumer health demands.

In conclusion, the production of carob syrup from thermally hydrolyzed integral carob flour stands as a significant advancement in the field of food innovation, offering promising opportunities for industrial application, improved resource efficiency, and the promotion of functional, nutritious, and eco-conscious food products.

CRediT authorship contribution statement

Ana Martins Vilas-Boas: Writing – review & editing, Writing – original draft, Validation, Software, Methodology, Investigation, Data curation, Conceptualization. **María Emilia Brassesco:** Writing – review & editing, Validation, Supervision, Software, Methodology, Investigation, Formal analysis. **Andreia C. Quintino:** Methodology, Investigation, Data curation. **Bruno Medronho:** Methodology, Investigation, Data curation. **Margarida C. Vieira:** Writing – review & editing, Visualization, Supervision. **Teresa R.S. Brandão:** Writing – review & editing, Visualization. **Cristina L.M. Silva:** Writing – review & editing, Visualization. **Beatriz Silva:** Methodology, Investigation. **Miguel Azevedo:** Writing – review & editing, Visualization. **Manuela Pintado:** Supervision, Project administration, Methodology, Conceptualization.

Informed consent statement

Not applicable.

Institutional review board statement

Not applicable.

Funding

This study is financed by Fundo Europeu de Desenvolvimento Regional (FEDER), through Programa Operacional Regional do Norte (PO Norte), in the scope of the Alphamais project: Development of new carob bean functional food ingredients (NORTE-01-0247-FEDER-039914). We would also like to thank the scientific collaboration under the FCT project UIDB/50016/2020

Declaration of competing interest

The authors declare that they have no known competing financial interests or personal relationships that could have appeared to influence the work reported in this paper.

Acknowledgments

We would like to thank all the help from our research group teammates, namely Manuela Machado for the expertise provided regarding the cellular model analyses.

Appendix A. Supplementary data

Supplementary data to this article can be found online at https://doi.org/10.1016/j.jfoodeng.2025.112767.

Data availability

Data will be made available on request.

References

Antunes, F., Andrade, F., Araújo, F., Ferreira, D., Sarmento, B., 2013. Establishment of a triple co-culture in vitro cell models to study intestinal absorption of peptide drugs. Eur. J. Pharm. Biopharm. 83 (3), 427–435.

AOAC, 1990. AOAC Official Methods of Analysis.

Baker, I., Chohan, M., Opara, E.I., 2013. Impact of cooking and digestion, in vitro, on the antioxidant capacity and anti-inflammatory activity of cinnamon, clove and nutmeg. Plant Foods Hum. Nutr. 68 (4), 364–369.

Ben Othmen, K., Elfalleh, W., García Beltrán, J.M., Esteban, M.Á., Haddad, M., 2020. An in vitro study of the effect of carob (*Ceratonia siliqua* L.) leaf extracts on gilthead seabream (*Sparus aurata* L.) leucocyte activities. Antioxidant, cytotoxic and bactericidal properties. Fish Shellfish Immunol. 99 (January 2019), 35–43.

Benković, M., Belščak-Cvitanović, A., Bauman, I., Komes, D., Srečec, S., 2017. Flow properties and chemical composition of carob (*Ceratonia siliqua* L.) flours as related to particle size and seed presence. Food Res. Int. 100 (July), 211–218.

Brand-Williams, W., Cuvelier, M.E., Berset, C., 1995. Use of a free radical method to evaluate antioxidant activity. LWT - Food Sci. Technol. (Lebensmittel-Wissenschaft -Technol.) 28 (1), 25–30.

Brassesco, M.E., Brandão, T.R.S., Silva, C.L.M., Pintado, M., 2021. Carob bean (*Ceratonia siliqua* L.): a new perspective for functional food. Trends Food Sci. Technol. 114 (June), 310–322.

Brassesco, M.E., Martins Vilas-Boas, A., Brandão, T.R.S., Silva, C.L.M., Azevedo, M., Pintado, M., 2023. Impact of roasting temperature and seed presence on carob flour (*Ceratonia siliqua* L.): physical, chemical, and functional properties. ACS Food Sci. Technol. 3 (11), 1890–1902.

Brodkorb, A., Egger, L., Alminger, M., Alvito, P., Assunção, R., Ballance, S., et al., 2019. INFOGEST static in vitro simulation of gastrointestinal food digestion. Nat. Protoc. 14 (4), 991–1014.

Chait, Y.A., Gunenc, A., Bendali, F., Hosseinian, F., 2020. Simulated gastrointestinal digestion and in vitro colonic fermentation of carob polyphenols: bioaccessibility and bioactivity. Lwt 117 (September 2019), 108623.

Coscueta, E.R., Pellegrini Malpiedi, L., Nerli, B.B., 2018. Micellar systems of aliphatic alcohol ethoxylates as a sustainable alternative to extract soybean isoflavones. Food Chem. 264 (May), 135–141.

Coscueta, E.R., Brassesco, M.E., Pintado, M., 2021. Collagen-based bioactive bromelain hydrolysate from salt-cured cod skin. Appl. Sci. (Switzerland) 11 (18).

Custódio, L., Fernandes, E., Escapa, A.L., Fajardo, A., Aligué, R., Alberício, F., et al., 2011. Antioxidant and cytotoxic activities of carob tree fruit pulps are strongly influenced by gender and cultivar. J. Agric. Food Chem. 59 (13), 7005–7012.

Da Silva, A.S.A., Espinheira, R.P., Teixeira, R.S.S., De Souza, M.F., Ferreira-Leitão, V., Bon, E.P.S., 2020. Constraints and advances in high-solids enzymatic hydrolysis of lignocellulosic biomass: a critical review. Biotechnol. Biofuels 13 (1), 1–28.

Derringer, G., Suich, R., 1980. Simultaneous optimization of several response variables. J. Qual. Technol. 12 (4), 214–219.

Dhaouadi, K., Belkhir, M., Akinocho, I., Raboudi, F., Pamies, D., Barrajón, E., et al., 2014. Sucrose supplementation during traditional carob syrup processing affected its chemical characteristics and biological activities. LWT - Food Sci. Technol. (Lebensmittel-Wissenschaft -Technol.) 57 (1), 1–8.

Edwards, C.H., Rossi, M., Corpe, C.P., Butterworth, P.J., Ellis, P.R., 2016. The role of sugars and sweeteners in food, diet and health: alternatives for the future. Trends Food Sci. Technol. 56, 158–166.

Erturk, M.Y., Le, A.N.M., Kokini, J., 2023. Advances in large amplitude oscillatory shear rheology of food materials. Front. Food Sci. Technol. 3.

Ghanemi, F.Z., Belarbi, M., Fluckiger, A., Nani, A., Dumont, A., De Rosny, C., et al., 2017. Carob leaf polyphenols trigger intrinsic apoptotic pathway and induce cell cycle arrest in colon cancer cells. J. Funct.Foods 33, 112–121.

Gómez-García, R., Sánchez-Gutiérrez, M., Freitas-Costa, C., Vilas-Boas, A.A., Campos, D. A., Aguilar, C.N., et al., 2022. Prebiotic effect, bioactive compounds and antioxidant capacity of melon peel (*Cucumis melo* L. inodorus) flour subjected to in vitro gastrointestinal digestion and human faecal fermentation. Food Res. Int. 154 (October 2021), 111045.

Gonçalves, B., Falco, V., Moutinho-Pereira, J., Bacelar, E., Peixoto, F., Correia, C., 2009. Effects of elevated CO2 on grapevine (*Vitis vinifera* L.): volatile composition, phenolic content, and in vitro antioxidant activity of red wine. J. Agric. Food Chem. 57 (1), 265–273.

Goulas, V., Hadjisolomou, A., 2019. Dynamic changes in targeted phenolic compounds and antioxidant potency of carob fruit (*Ceratonia siliqua* L.) products during in vitro digestion. Lwt 101, 269–275. October 2018.

Gunel, Z., Torun, M., Sahin-Nadeem, H., 2020. Sugar, d-pinitol, volatile composition, and antioxidant activity of carob powder roasted by microwave, hot air, and combined microwave/hot air. J. Food Process. Preserv. 44 (4), 1–10.

Gunst, R.F., 1996. Response surface methodology: process and product optimization using designed experiments. Technometrics 38 (3), 284–286.

Infurna, G., Botta, L., Maniscalco, M., Morici, E., Caputo, G., Marullo, S., et al., 2022. Biochar particles obtained from agricultural carob waste as a suitable filler for sustainable biocomposite formulations. Polymers 14 (15).

ISO, 2009. International Organization for Standardization. https://www.iso.org/.

ISO, 2013. International Organization for Standardization. https://www.iso.org/.

Jakobek, L., 2015. Interactions of polyphenols with carbohydrates, lipids and proteins. Food Chem. 175, 556–567.

Lee, J.W., Thomas, L.C., Schmidt, S.J., 2011. Can the thermodynamic melting temperature of sucrose, glucose, and fructose be measured using rapid-scanning differential scanning calorimetry (DSC)? J. Agric. Food Chem. 59 (7), 3306–3310.

Loow, Y.L., Wu, T.Y., Md, Jahim, J., Mohammad, A.W., Teoh, W.H., 2016. Typical conversion of lignocellulosic biomass into reducing sugars using dilute acid hydrolysis and alkaline pretreatment. Cellulose 23 (3), 1491–1520.

Loullis, A., Pinakoulaki, E., 2018. Carob as cocoa substitute: a review on composition, health benefits and food applications. Eur. Food Res. Technol. 244 (6), 959–977.

Luo, X., Wang, Q., Fang, D., Zhuang, W., Chen, C., Jiang, W., et al., 2018. Modification of insoluble dietary fibers from bamboo shoot shell: structural characterization and functional properties. Int. J. Biol. Macromol. 120, 1461–1467.

Ma, M., Mu, T., 2016. Modification of deoiled cumin dietary fiber with laccase and cellulase under high hydrostatic pressure. Carbohydr. Polym. 136, 87–94.

Mahtout, R., Zaidi, F., Ould Saadi, L., Boudjou, S., Oomah, B.D., Hosseinian, F., 2016. Carob (*Ceratonia siliqua* L.) (pod, pulp, seed) flours and pulp mucilage affect kefir quality and antioxidant capacity during storage. Int. J. Eng. Tech. 2 (2), 118–180.

Martínez-Las Heras, R., Pinazo, A., Heredia, A., Andrés, A., 2017. Evaluation studies of persimmon plant (*Diospyros kaki*) for physiological benefits and bioaccessibility of antioxidants by in vitro simulated gastrointestinal digestion. Food Chem. 214, 478–485.

Nagib, K., Eldahshan, O.A., El-Khatib, W.F.A.M., 2010. Promising antioxidant and cytotoxic activities of the aqueous ethanolic extract of carob leaves. Afr J Pharm Pharmacol 4 (6), 330–334.

Nasar-abbas, S.M., Vu, T.H., Khan, M.K., Esbenshade, H., Jayasena, V., 2016. Carob kibble : a bioactive-rich food ingredient. Compr. Rev. Food Sci. Food Saf. 15, 63–72.

Norma NP 518, 1986. Norma Portuguesa.

Özcan, M.M., Arslan, D., Gökçalik, H., 2007. Some compositional properties and mineral contents of carob (*Ceratonia siliqua*) fruit, flour and syrup. Int. J. Food Sci. Nutr. 58 (8), 652–658.

Papaefstathiou, E., Agapiou, A., Giannopoulos, S., Kokkinofta, R., 2018. Nutritional characterization of carobs and traditional carob products. Food Sci. Nutr. 6 (8), 2151–2161.

Polanowska, K., Varghese, R., Kuligowski, M., Majcher, M., 2021. Carob kibbles as an alternative raw material for production of kvass with probiotic potential. J. Sci. Food Agric. 101 (13), 5487–5497.

Qi, J., Yokoyama, W., Masamba, K.G., Majeed, H., Zhong, F., Li, Y., 2015. Structural and physico-chemical properties of insoluble rice bran fiber: effect of acid-base induced modifications. RSC Adv. 5 (97), 79915–79923.

Rahman, J.M.H., Shiblee, M.N.I., Ahmed, K., Khosla, A., Kawakami, M., Furukawa, H., 2020. Rheological and mechanical properties of edible gel materials for 3D food printing technology. Heliyon 6 (12), e05859.

Rico, D., Martín-Diana, A.B., Martínez-Villaluenga, C., Aguirre, L., Silván, J.M., Dueñas, M., et al., 2019. In vitro approach for evaluation of carob by-products as source bioactive ingredients with potential to attenuate metabolic syndrome (MetS). Heliyon 5 (1), e01175.

Rodríguez-Solana, R., Coelho, N., Santos-Rufo, A., Gonçalves, S., Pérez-Santín, E., Romano, A., 2019. The influence of in vitro gastrointestinal digestion on the chemical composition and antioxidant and enzyme inhibitory capacities of carob liqueurs obtained with different elaboration techniques. Antioxidants 8 (11).

Rodríguez-Solana, R., Romano, A., Moreno-Rojas, J.M., 2021. Carob pulp: a nutritional and functional By-Product worldwide spread in the formulation of different food products and beverages. A review. Processes 9 (7), 1146.

Saitta, F., Apostolidou, A., Papageorgiou, M., Signorelli, M., Mandala, I., Fessas, D., 2023. Influence of carob flour ingredients on wheat-based systems. J. Cereal. Sci. 111 (September 2022), 103655.

Vilas-Boas, A.M., Brassesco, M.E., Quintino, A.C., Vieira, M.C., Brandão, T.R.S., Silva, C. L.M., et al., 2022. Particle size effect of integral carob flour on bioaccessibility of bioactive compounds during simulated gastrointestinal digestion. Foods 11 (9), 1272.

Wang, Y., Truong, T., Li, H., Bhandari, B., 2019. Co-melting behaviour of sucrose, glucose & fructose. Food Chem. 275 (August 2018), 292–298.

Wootton-Beard, P.C., Moran, A., Ryan, L., 2011. Stability of the total antioxidant capacity and total polyphenol content of 23 commercially available vegetable juices before and after in vitro digestion measured by FRAP, DPPH, ABTS and Folin-Ciocalteu methods. Food Res. Int. 44 (1), 217–224.

Ydjedd, S., Bouriche, S., López-Nicolás, R., Sánchez-Moya, T., Frontela-Saseta, C., Ros-Berruezo, G., et al., 2017. Effect of in vitro gastrointestinal digestion on encapsulated and nonencapsulated phenolic compounds of carob (*Ceratonia siliqua* L.) pulp extracts and their antioxidant capacity. J. Agric. Food Chem. 65 (4), 827–835.

Yu, G., Bei, J., Zhao, J., Li, Q., Cheng, C., 2018. Modification of carrot (*Daucus carota* Linn. var. Sativa Hoffm.) pomace insoluble dietary fiber with complex enzyme method, ultrafine comminution, and high hydrostatic pressure. Food Chem. 257 (17), 333–340.

Zhang, M.Y., Liao, A.M., Thakur, K., Huang, J.H., Zhang, J.G., Wei, Z.J., 2019. Modification of wheat bran insoluble dietary fiber with carboxymethylation, complex enzymatic hydrolysis and ultrafine comminution. Food Chem. 297 (June).

Zhu, B.J., Zayed, M.Z., Zhu, H.X., Zhao, J., Li, S.P., 2019. Functional polysaccharides of carob fruit: a review. Chin. Med. 14 (1), 1–10.